

# Functionalization of Polylactic Acid Through Direct Melt Polycondensation in the Presence of Tricarboxylic Acid

Pavel Kucharczyk,<sup>1</sup> Ida Poljansek,<sup>2,3</sup> Vladimír Sedlarik,<sup>1,4</sup> Vera Kasparkova,<sup>5</sup>  
Alexandra Salakova,<sup>6</sup> Jan Drbohlav,<sup>6</sup> Uros Cvelbar,<sup>4</sup> Petr Saha<sup>1</sup>

<sup>1</sup>Centre of Polymer Systems, Polymer Centre, Tomas Bata University in Zlin, 760 01 Zlin, Czech Republic

<sup>2</sup>National Institute of Chemistry, Hajdrihova 19, 1000 Ljubljana, Slovenia

<sup>3</sup>Centre of Excellence Polymer Materials and Technologies, 1000 Ljubljana, Slovenia

<sup>4</sup>Jozef Stefan Institute, 1000 Ljubljana, Slovenia

<sup>5</sup>Department of Fat, Tenside and Cosmetics Technology, Faculty of Technology, Tomas Bata University in Zlin, 76272 Zlin, Czech Republic

<sup>6</sup>Milcom a.s. Ke Dvoru 12a, 16000 Prague, Czech Republic

Received 8 July 2010; accepted 30 January 2011

DOI 10.1002/app.34260

Published online 21 May 2011 in Wiley Online Library (wileyonlinelibrary.com).

**ABSTRACT:** The goal of the article was to describe the preparation of carboxyl-functionalized polylactic acid (PLA) through the method of direct melt copolycondensation of lactic and citric acid (CA). In addition, detailed study of copolycondensation process, its limitations and investigation of the reaction products properties are another issue this article deals with. The effect of tricarboxylic CA on the resulting properties of the functionalized lactic acid (LA) polycondensates was studied in a wide range of LA/CA molar ratios. The influence of CA on molecular weight, thermal and physicochemical properties, and chemical structure of the products was investigated, using viscometric measurements of the polymer solutions, gel permeation chromatography, <sup>1</sup>H nuclear magnetic resonance spectroscopy, differential scanning calorimetry,

acidity number determination, and Fourier-transform infrared and ultraviolet spectroscopy. The results show the significant effect of CA on the structure and physicochemical properties as well as high efficiency of functionalization. Furthermore, a branched structure was detected at low CA concentrations, while higher CA content leads to termination of the polycondensates chains by citryl units and a reduction in the molecular weight. Here, insights on the characterization methods of PLA-based materials are given by various experimental techniques. © 2011 Wiley Periodicals, Inc. *J Appl Polym Sci* 122: 1275–1285, 2011

**Key words:** functionalization of polymers; biodegradable; polyesters; synthesis; gel permeation chromatography (GPC)

## INTRODUCTION

In recent years, biodegradable polymers have been investigated extensively for their potential applications in medical and pharmaceutical fields.<sup>1–4</sup> Polylactic acid (PLA) is one of the promising biodegradable polymers, which belongs to the group of aliphatic polyesters. The excellent properties of PLA

and its copolymers, such as biodegradability and biocompatibility, predetermine them to be used for medical devices (sutures, bone fixations, and implants) and also drug carriers (nano- and microparticles and polymer–drug conjugates) as reported in many publications.<sup>5–8</sup> In addition, there are other nonmedical areas of PLA use, which are objects of both scientific and practical use interest due the possibility of PLA production based on environmental friendly technologies availing renewable materials (biodegradable packaging, materials based on renewable resources).<sup>3,9,10</sup>

The demands made on the materials applied especially in medical area (biocompatibility, improved polymer–organism interaction, and functionality) lead to the subsequent necessity for further modifications of PLA.<sup>11</sup> The process of copolymerization has been already indicated above. It represents the most effective of PLA modifications in bulk. Many works dealing with preparation of lactic acid (LA)/glycolic acid copolymers have been reported.<sup>12,13</sup> The introduction of hydroxyl groups into PLA chains has been described by copolymerization of

Correspondence to: V. Sedlarik (sedlarik@ft.utb.cz).

Contract grant sponsor: Ministry of Education, Youth and Sports of the Czech Republic; contract grant number: 2B08071.

Contract grant sponsor: European Regional Development Fund; contract grant number: CZ.1.05/2.1.00/03.0111.

Contract grant sponsor: Ministry of Higher Education, Science and Technology of the Republic of Slovenia; contract grant numbers: P2-0145, P4-0015-0481.

Contract grant sponsor: Slovenian Research Agency (ARRS); Science and Education Foundation of the Republic of Slovenia.

LA with, e.g., polyethylene glycol.<sup>14</sup> The introduction of thiol groups into PLA chain ends can be mentioned as another example.<sup>15</sup> On the other hand, effective surface modifications can be achieved by plasmatic treatment of a polymer.<sup>16–18</sup> In case of PLA, noticeable improvement of surface biocompatibility has been obtained, for instance, by ammonia plasma treatment.<sup>19,20</sup>

This work is dedicated to the preparation of PLA-based copolymers with an increased amount of carboxyl functional groups. It is done by copolymerization of LA with, tricarboxylic, citric acid (CA) by direct polycondensation of LA and CA in the molten state. The resulting product, poly(L-lactic acid-*co*-citric acid) (PLACA) is expected to have improved interactions with living systems.<sup>21</sup> In addition, the introduction of carboxyl provides the eventuality for further functionalization of the material through immobilizing or entrapping of bioactive species.<sup>17</sup> The preparation of PLACA oligomer prepared by direct polycondensation has been already published by Yao et al.<sup>21</sup> However, his work concentrates only on two comonomer molar ratios (12 : 1 and 24 : 1). The reaction was catalyzed by stannous chloride in this work. The product of reaction has a molecular weight below 1500 and 2200 g mol<sup>-1</sup> for ratios 12 : 1 and 24 : 1, respectively (determined by GPC). It is clear that these materials are not suitable for load-bearing medical applications such as orthopedic implants because of their weak mechanical properties as a consequence of low-molecular weight. On the other hand, functionalized low-molecular weight polylactide and its copolymers can find their use in the areas where high-mechanical performance is not needed and where the main stress is put on chemical properties of the materials. Encapsulation<sup>22,23</sup> and coating<sup>24</sup> techniques or tissue adhesives<sup>25</sup> can be mentioned as an example. In addition, the presence of reactive groups in the polylactide structure offers a possibility for chain-linking reactions. For instance, Yao's group have further described the preparation of multiblock copolymer based on LA/CA copolycondensate and polyethylene glycol (10,000 g mol<sup>-1</sup>). The product of the reaction proved molecular weight over 75,000 g mol<sup>-1</sup>.<sup>26</sup>

Despite the polycondensation of the LA and CA has been already investigated<sup>21</sup> several, from the practical applicability point of view, questions remains to be answered. First, it is necessary to determine the maximal possible extend of PLA functionalization by carboxyl groups by the polycondensation method. Second, the effect of functionalization on the reaction product properties needs to be described. Last but not least, the structural parameters should be known for the purpose of the further intended application in the field of bioactive materials preparation. Keeping these facts in mind, the aim

of this study is to prepare and characterize the PLACA by direct melt polycondensation of LA and CA at high CA comonomer concentrations (0–20 wt %, i.e., LA:CA molar ratio from 9 : 1 up to 211 : 1). The crucial attention is paid to the determination of carboxyl functionalization on structural properties by using gel permeation chromatography (GPC), <sup>1</sup>H nuclear magnetic resonance (<sup>1</sup>H NMR), and Fourier-transform infrared (FTIR) spectroscopy. The observed results are correlated with thermal, viscometric, and acid–base properties of the copolycondensates by differential scanning calorimetry (DSC), viscometric measurements of polymer solutions, and titrimetric determination of carboxyl groups.

## EXPERIMENTAL

### Materials

L-LA C<sub>3</sub>H<sub>6</sub>O<sub>3</sub>, 80% water solution, optical rotation [ $\alpha$ ] = 10.6° (measured by the polarimeter Optech P1000 at 22°C, concentration of 10%) was purchased from Lachner Neratovice, Czech Republic. Stannous 2-ethylhexanoate (Sn(Oct)<sub>2</sub>) (~ 95%), dimethyl sulfoxide C<sub>2</sub>H<sub>6</sub>OS in deuterated form (DMSO-*d*<sub>6</sub>) (100 mol % purity) and tetramethylsilane C<sub>4</sub>H<sub>12</sub>Si (TMS) were supplied by Sigma Aldrich, Steinheim, Germany. The solvents acetone C<sub>3</sub>H<sub>6</sub>O, dichloromethane CH<sub>2</sub>Cl<sub>2</sub>, methanol CH<sub>4</sub>O, ethanol C<sub>2</sub>H<sub>6</sub>O, indicator bromothymol blue C<sub>27</sub>H<sub>28</sub>Br<sub>2</sub>O<sub>5</sub>S, potassium hydroxide KOH, and anhydrous CA C<sub>6</sub>H<sub>8</sub>O<sub>7</sub> (all analytical grade) were bought from IPL Lukes, Uhersky Brod, Czech Republic. Chloroform CHCl<sub>3</sub> (HPLC grade) was purchased Chromspec, Brno, Czech Republic. All chemicals were used as obtained without further purification.

### Polycondensation

A typical procedure was as follows: relevant portions of LA and CA (0, 1, 3, 5, 7, 10, 15, and 20 wt %-related to LA) were added into a double-necked flask (250 mL) equipped with a Teflon stirrer. Total mass of the mixture at the beginning of reaction was 50 g (water is not included). The flask was then placed in an oil bath heated by magnetic stirrer with heating and connected to a laboratory apparatus for distillation under reduced pressure. The dehydration step followed at 160°C, reduced pressure 15 kPa for 4 h. After that, the reactor was disconnected from the vacuum pump and the relevant amount (0.5 wt %, related to initial mass of the reactants) of the catalyst (Sn(Oct)<sub>2</sub>) was added dropwise under continuous stirring. The flask with dehydrated LA/CA/catalyst mixture was connected back to the source of vacuum (100 Pa) and the reaction continued for 24 h at the temperature 160°C. The resulting product was

allowed to cool down at room temperature and then dissolved in acetone. The polymer solution was precipitated in a mixture of chilled methanol/distilled water 1 : 1 (v/v). The obtained product was filtrated, washed with methanol, and dried at 45°C for 48 h. The dissolving-precipitation procedure was repeated three times. The pH value of the filtrate after polymer separation was checked to ensure that an unreacted CA is not present in the polymer.

## Characterization methods

### Viscometric measurements

Viscosity measurements were performed in chloroform at 30°C in an Ubbelohde viscometer with capillary 0a. The intrinsic viscosity,  $[\eta]$ , was calculated using the eq. (1):

$$[\eta] = \lim_{c \rightarrow 0} \frac{\eta_{\text{rel}} - 1}{c} \quad (1)$$

where  $\eta_{\text{rel}}$  is the relative viscosity, which is equal to the ratio of polymer solution and pure solvent viscosities, and  $c$  is the concentration of the polymer solution (0.4, 0.8, and 1.2 w/v %).

### Determination of molecular weight by GPC

GPC analyses were performed using a chromatographic system Breeze (Waters) equipped with a PLgel Mixed-D column (300 × 7.8 mm<sup>2</sup>, 5 μm) (Polymer Laboratories, Church Stretton, United Kingdom). For detection, a Waters 2487 Dual absorbance detector at 239 nm was employed. Analyses were carried out at room temperature with a flow rate of 1.0 mL min<sup>-1</sup> in chloroform. The column was calibrated using narrow molecular weight polystyrene standards with molar mass ranging from 580 to 480,000 g mol<sup>-1</sup> (Polymer Laboratories). A 100-μL injection loop was used for all measurements. The sample concentration ranged from 1.6 to 2.2 mg mL<sup>-1</sup>. Data processing was carried out using the Waters Breeze GPC Software (Waters). The weight average molar mass  $M_w$ , number average molar mass  $M_n$ , and polydispersity ( $M_w/M_n$ ) of the tested samples were determined.

### Fourier-transform infrared spectroscopy

Functional groups in LA polycondensation products were identified using FTIR analysis. The investigation was conducted on NICOLET 320 FTIR, equipped with attenuated total reflectance (ATR) accessory utilizing Zn-Se crystal and the software package OMNIC over the range of 4000–650 cm<sup>-1</sup> at room temperature. The uniform resolution of 2 cm<sup>-1</sup> was maintained in all cases.

### Differential scanning calorimetry

For the determination of glass transition temperature ( $T_g$ ), melting point ( $T_m$ ), and crystallinity ( $\chi_c$ ) of the polycondensates, the DSC was used. Approximately 8 mg of the sample was placed in an aluminum pan, sealed, and analyzed on NETZSCH DSC 200 F3, calibrated in terms of temperature and heat flow, using indium. The experiments were performed under nitrogen atmosphere (60 mL min<sup>-1</sup>) in two scans in the temperature range of 0–180°C and at the heating rate of 10°C min<sup>-1</sup>. Crystallinity (%),  $\chi_c$ , was estimated by the following equation:

$$\chi_c = \frac{\Delta H_m}{\Delta H_m^0} \times 100 \quad (2)$$

where,  $\Delta H_m^0$  is the enthalpy of melting for 100% crystalline PLA (93.7 J g<sup>-1</sup>) adopted from Fischer et al.<sup>27</sup> and  $\Delta H_m$  represents the measured melting enthalpy of the sample taken from the first heating scan.

### <sup>1</sup>H Nuclear magnetic resonance

The composition of the selected polycondensation products (PLA, PLACA1%, PLACA 5%, and PLACA 20%), as well as the component structure, was determined with <sup>1</sup>H NMR spectroscopy using a Unity Inova 300 Varian NMR spectrometer operating at 300 MHz. The sample concentration was 1% (w/w) in the solvent DMSO-*d*<sub>6</sub> (Aldrich, 100.0 mol % purity). All the spectra were obtained at 25°C using 5-mm glass NMR tubes, and TMS as the internal standard. The conditions for the <sup>1</sup>H NMR were as follows: a 90° pulse angle, a 5-s delay between the pulses, an acquisition time of 5 s, and up to 32 repetitions. VNMRJ rev. 1.1D software was applied for the peak integration. The lactic-to-citric monomer ratio and the number molecular weight were calculated according to the procedure described by Yao et al.<sup>21</sup>

### Acidity number determination

The concentration of terminal carboxyl groups was expressed as acidity number (AN), which represents the amount of KOH (in milligrams) for neutralization of 1 g of a substance. AN was determined by titration of the sample in methanol/dichloromethane (1 : 1 v/v) with 0.01M KOH ethanol solution. Bromothol blue was used as an indicator.<sup>21</sup>

### Spectroscopy in ultraviolet light spectrum

The spectroscopic analysis of the samples in ultraviolet and part of the visible range of light was

TABLE I  
Characteristics of PLACA Polycondensates

Sample designation	$M_n^a$ (kg mol <sup>-1</sup> )	$M_w^a$ (kg mol <sup>-1</sup> )	$M_w/M_n^a$	$[\eta]^b$ (dL g <sup>-1</sup> )	Yield <sup>c</sup> (wt %)	AN/SD <sup>d</sup> (mg <sub>KOH</sub> g <sup>-1</sup> )	Appearance
PLA	22.6	46.9	2.1	0.47	62	23.6/1.9	White powder
PLACA 1%	10.8	27.0	2.5	0.25	46	30.0/1.5	Yellowish powder
PLACA 3%	1.9	7.7	4.1	0.20	25	35.7/1.7	Yellowish powder
PLACA 5%	1.1	4.7	4.3	0.14	22	50.5/1.2	Yellowish powder
PLACA 7%	0.9	4.0	4.4	0.15	53	54.0/1.3	Yellow powder
PLACA 10%	0.3	1.4	4.7	0.09	33	78.6/1.2	Waxy-light brown
PLACA 15%	0.2	1.2	6.0	0.08	43	98.4/1.7	Waxy-light brown
PLACA 20%	0.2	1.2	6.0	0.08	48	97.9/1.1	Waxy-light brown

<sup>a</sup> GPC analysis.

<sup>b</sup> Viscometry (30°C in CHCl<sub>3</sub>).

<sup>c</sup> Calculated on the basis of copolycondensation product mass after precipitation procedure.

<sup>d</sup> SD, standard deviation.

conducted on the prepared samples to reveal functionalization extend of the polycondensates with carboxyl groups. The samples were dissolved in chloroform to form a polymer solution (~ 0.1 mg/mL). The analysis was carried out by Helios Gamma UV-Visible spectrometer in a quartz cuvette (path length, 10 mm) over the wavelength range 200–400 nm with resolution 0.5 nm at room temperature.

## RESULTS AND DISCUSSION

The basic characteristics of the samples prepared by melt polycondensation of LA and CA are shown in Table I. It can be noticed that the increasing content of CA in the reaction mixture leads (beside the visual change of the product) to significant reduction of  $[\eta]$ . While the pure PLA has  $[\eta] = 0.47$  dL g<sup>-1</sup>, PLACA 5% in the mixture causes noticeable reduction of  $[\eta]$ , which possesses >55% of the value obtained for pure PLA. However, noticeable reduction of  $[\eta]$  was observed already for PLACA 1% (>45%). The samples that were prepared in above 10 wt % CA presence are characteristic with low  $[\eta]$ , which corresponds to their waxy-like appearance unlike the powder form of the polycondensation products prepared at lower concentration of tricarboxylic acid.

The values of molecular weight determined by GPC (Table I) correspond to the intrinsic viscosity data. The highest  $M_w$  was achieved in case of PLA (46,900 g mol<sup>-1</sup>). The increasing content of CA in the reaction mixture decreases  $M_w$  steeply. Finally, the sample designated as PLACA 20% proves  $M_w$  of only 1200 g mol<sup>-1</sup>. In addition, polydispersity ( $M_w/M_n$ ) of the polycondensates increases from 2.1 (for PLA) to 6.0 (for PLACA 20%). These results reveal the possible integration of CA into the PLA chain during polycondensation process, which can be supported by the assumption that higher volume resistance corresponds to lower reactivity of CA. It

means that CA molecules rather do not react with each other. On the other hand, when LA or its oligomer reacts with one of the CA functional groups, it would be arduous for such molecule to undergo further condensation reaction because of the reasons mentioned above.<sup>21</sup> Moreover, CA contains three carboxylic and one hydroxyl group while LA possesses one from each. Thus the ratio COOH/OH is shifted toward values higher than 1 in the presence of CA in the reaction mixture. The reduction of molecular weight and the increasing polydispersity index is a logical consequence of that.

The incorporation of CA into the structure of a product through condensation reaction can be proved by the determination of carboxyl groups, which should be in excess in case the reaction took place during product formation. The titration method can provide such information in the form of AN as presented above. This method is considered to be a reliable tool for the determination of molecular weight of a polymer (end-groups determination). However, it cannot be used in case of PLACA polycondensates due to several reasons. First, PLA itself is not considered to be terminated by carboxyl groups. Second, the results indicate possible incorporation of citryl units into the structure of PLACA at lower CA concentration in the feed (see further). The values of AN, shown in Table I, are in accordance of the assumption of occurrence of the condensation reaction between LA and CA molecules. Despite the already mentioned assumption of carboxyl absence in the pure PLA, small AN was observed (26 mg KOH g<sup>-1</sup>). It can be ascribed to the presence of residual monomer. In addition, the indicator, bromothylol blue, has equivalence point above pH 7. The rising CA content causes an increase in AN up to 15 wt % CA in reaction mixture. The AN values for PLACA 15% and PLACA 20% are more or less identical, which reveals possible limits of CA incorporation into the structure of the product. This limit is



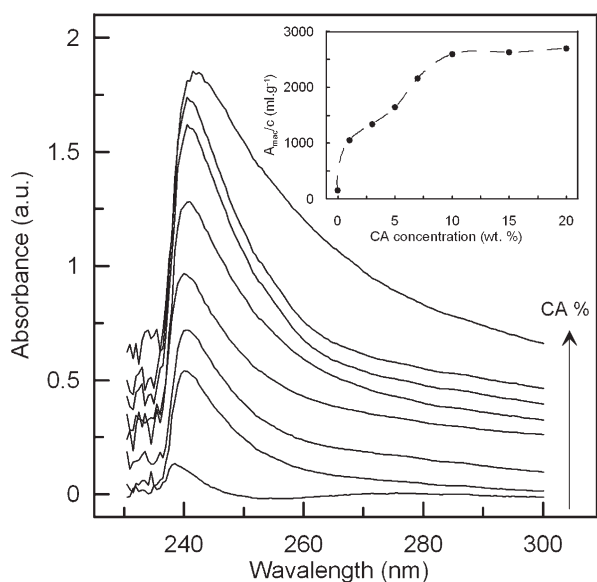


**Figure 1** UV spectra of PLA and PLACA polycondensates. Embedded figure shows dependence of  $A_{\max}$  normalized with respect to the sample concentration on CA content in the feed.

connected with the inhibition of condensation reaction that leads to reduction of molecular weight of the samples (Table I). It can be supposed that this method considers mostly the carboxyl groups appearing at the end of polymeric chains. The amount of such terminations increases with the increasing amount of short chains of the polymer or its branches. It should be mentioned that the yields shown in Table I represent pure yield of the polycondensation products after purification process described in the sample preparation section.

UV-Vis analysis of the samples can support the idea of COOH attachment on PLA chains. Generally, PLA shows maximal absorbance at wavelength ( $\lambda_{\max}$ ) 240 nm.<sup>8</sup> In our case, pure PLA proved  $\lambda_{\max} = 237$  nm. The increasing content of CA led to slight shift of  $\lambda_{\max}$  toward higher values. The sample with the highest investigated CA content in the feed (PLACA 20%) shows  $\lambda_{\max} = 242$  nm. Figure 1 shows spectra of the PLA and PLACA chloroform solutions within the range of 200–400 nm. It can be noticed that the absorption at  $\lambda_{\max}$  increases with rising content of CA. It can be considered that this phenomenon is a consequence of PLA functionalization. The embedded figure shows dependence of maximal absorption ( $A_{\max}$ ) normalized with the concentration of polymer in the solution,  $c$  ( $\text{g mL}^{-1}$ ) on CA concentration. It clearly shows that the most significant functionalization degree is proceeded up to 10 wt % of CA. Further additions of CA do not enhance  $A_{\max}/c$  value, which is proved by a plateau occurrence. These results are in full agreement with AN determination (see Table I).

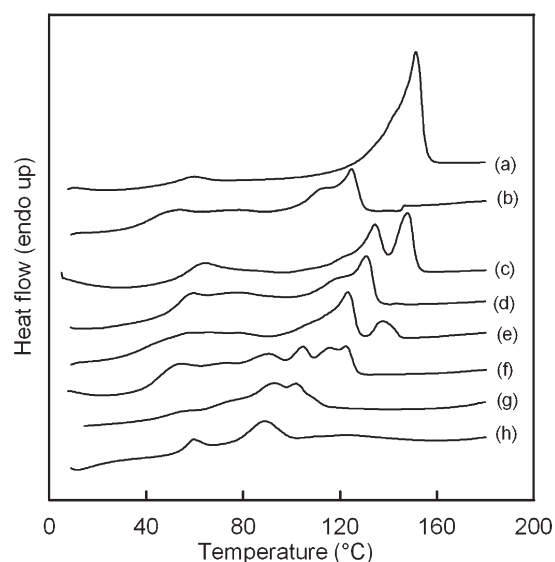


**Figure 2** DSC curve of polycondensates—first heating scan: (a) PLA, (b) PLACA 1%, (c) PLACA 3%, (d) PLACA 5%, (e) PLACA 7%, (f) PLACA 10%, (g) PLACA 15%, and (h) PLACA 20%.

The DSC spectra thermograms of the samples obtained from the first heating scan are shown in Figure 2 and the observed characteristics (melting point and melting enthalpy) are summarized in Table II. All samples containing CA proved double melting exothermic peaks while pure PLA is distinguished by a significant single melting peak situated at 151.2 °C with melting enthalpy 48.9  $\text{J g}^{-1}$ . The phenomenon of cold crystallization was not observed. Similar results have been reported by Yao et al.<sup>21</sup> Generally, CA presence decreases  $T_m$  of the samples and this reduction corresponds to the CA concentration in the system [Fig. 2(b–h)]. The only exception is created by PLACA 1%, which shows a noticeably lower  $T_{m1}$  and  $T_{m2}$ . The experiment was conducted multiple times with similar results [Fig. 2(b)]. The reason of such behavior could be found in possible obstruction of the volume of CA molecules during development of organized polymer units. This may be possible under the condition that some of the CA

**TABLE II**  
DSC Characteristics of the PLA and PLACA Samples  
(First Heating Scan)

Sample designation	$T_{m1}$ (°C)	$\Delta H_{m1}$ ( $\text{J g}^{-1}$ )	$T_{m2}$ (°C)	$\Delta H_{m2}$ ( $\text{J g}^{-1}$ )
PLA	151.2	48.9	—	—
PLACA 1%	110.0	12.73	124.8	16.8
PLACA 3%	134.5	11.82	147.9	16.9
PLACA 5%	118.1	7.65	130.9	17.4
PLACA 7%	123.4	11.95	137.6	4.8
PLACA 10%	104.4	4.6	122.3	10.9
PLACA 15%	90.1	3.9	102.0	8.9
PLACA 20%	59.1	2.9	88.5	7.6

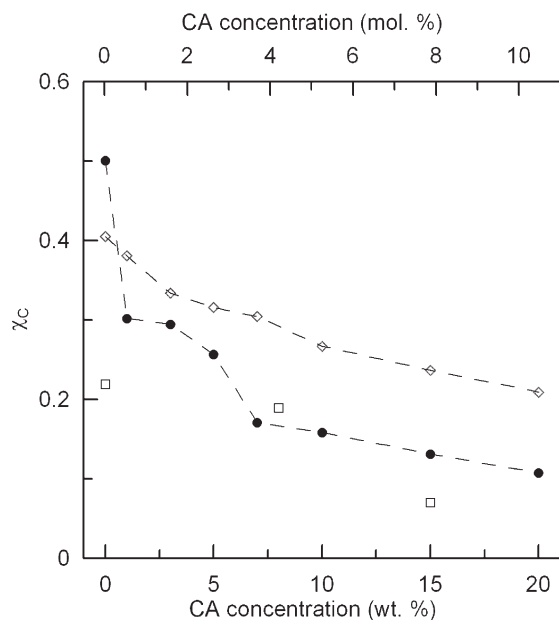


**Figure 3** Effect of CA concentration on crystallinity of the PLACA polycondensates determined by DSC (filled symbols) and FTIR (empty symbols) techniques. Square symbols represent data (DSC) published by Yao et al.<sup>21</sup>

molecules (present in low amount in case of PLACA 1%) is incorporated inside of the polymer chain; i.e., it does not terminate the chain. On the other hand, the polycondensation inhibition effect becomes predominant at higher concentrations of CA as a result of termination of polycondensate chains by sterically bulky citryl groups. Increasing content of CA in the feed obviously increasing the probability of that. This effect could be predominant here rather than excess of COOH groups. It is connected with the decreasing molecular mass (Table I),  $T_m$  and  $\Delta H_m$  (Table II). The effect of CA presence on crystallinity ( $\chi_c$ ) calculated according eq. (1) is shown in Figure 3. The dashed guiding line connecting individual experimental points clearly indicates that  $\chi_c$  decreases significantly at the lowest investigated addition of CA into reaction mixture (1 wt %). Further increase in CA concentration (up to 7 wt %) is characterized by a decrease of  $\chi_c$  values. However, it is not as steep as in the previous case and graphical depiction has a convex shape. The  $\chi_c$  reduction was observed to be gradual in case of the samples with higher CA contents (above 10 wt %), where the effect of CA presence becomes less significant.

Second DSC heating scans are shown in Figure 4. The positions of the midpoint stepwise increase of the specific heat provide the values of glass transition temperature ( $T_g$ ) of the samples (Fig. 4). On the other hand, the endothermic peaks revealing melting were diminished with incorporation of citryl units into the polycondensates structure, due to significant reduction of the PLACA chain ability to be organ-

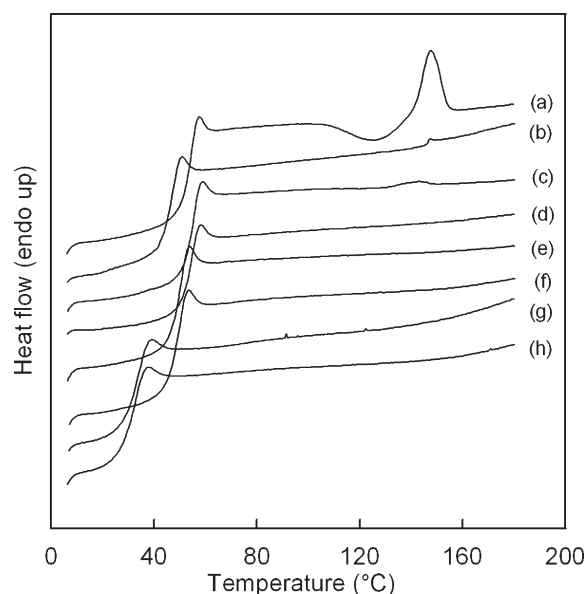


**Figure 4** DSC curve of polycondensates—second heating scan: (a) PLA, (b) PLACA 1%, (c) PLACA 3%, (d) PLACA 5%, (e) PLACA 7%, (f) PLACA 10%, (g) PLACA 15%, and (h) PLACA 20%.

ized into crystalline units. The dependence of  $T_g$  on CA concentration is depicted in Figure 5. As well as in the case of melting behavior, the  $T_g$  decreases with rising CA presence. The decrease is gradual and the difference between PLA and PLA with the highest investigated amount of CA (PLACA 20%) is almost 21.5°C. These experimental results fit well to

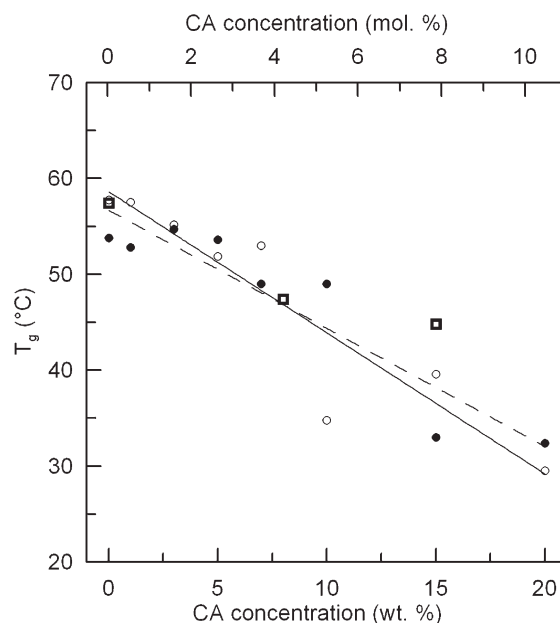


**Figure 5** Glass transition temperature ( $T_g$ ) versus CA concentration (experimental data—full symbols and solid line fit, theoretical data—empty symbols and dashed line fit). Square symbols represent data published by Yao et al.<sup>21</sup>

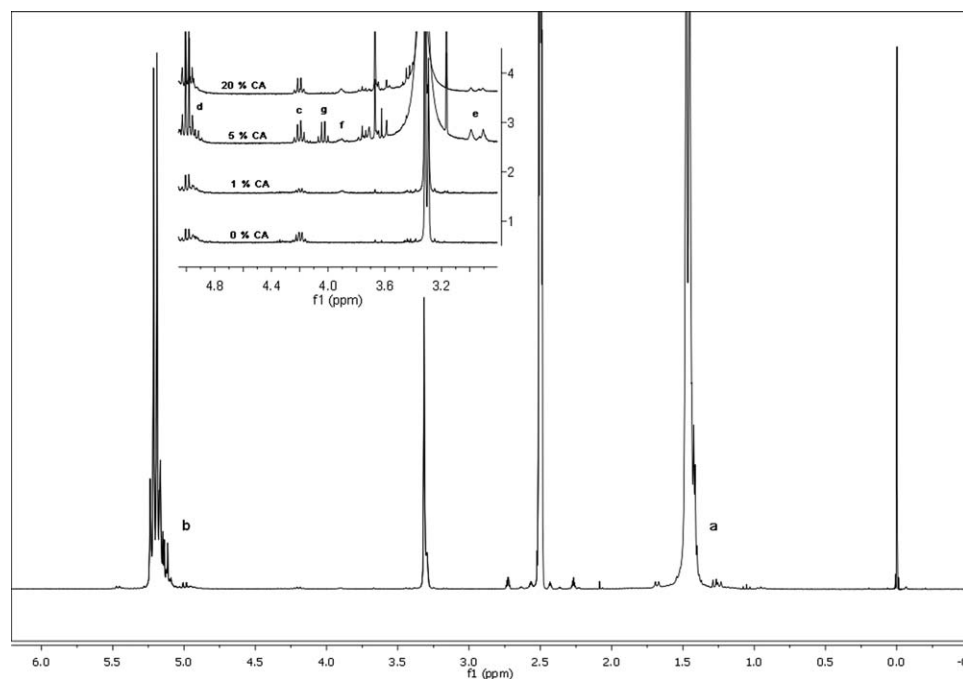


**Figure 6**  $^1\text{H}$  NMR spectra of the selected polycondensates. The master curve belongs to PLACA 1%.

theoretical predictions of  $T_g$ , which was performed according to Fox-Flory;

$$T_g = T_g^\infty - \frac{K}{M_n} \quad (3)$$

where  $T_g^\infty$  represents the glass transition temperature at an infinite molecular weight of polymer, and  $K$  is a constant representing the excess free volume of the polymer chains end groups.  $M_n$  was taken from GPC measurements (Table I). Jashimi et al. reported  $T_g^\infty = 58^\circ\text{C}$  and  $K = 5.5 \times 10^4$  (for low-crystalline PLA).<sup>28</sup> We have already informed that eq. (3) fails at low  $M_n$  of PLA.<sup>3</sup> Interestingly, the relation between  $T_g$  and  $M_n$  is relatively valid for PLACA samples even at low-molecular weights of the polycondensation products obtained at higher CA concentrations. The only significant deviation between experimental and theoretical  $T_g$  was observed for PLACA 10%. Nevertheless, these calculations are strongly dependent on  $M_n$  determination and their accuracy is in orders of hundreds of gram per mole in case of GPC. On the other hand, simplification by means of linear fitting of both experimental and theoretical data (solid and dashed lines in Fig. 5) may be considered acceptable for preliminary  $T_g$  estimation of the given material.

As already mentioned, polycondensation of LA and CA has been already reported by Yao et al.<sup>21</sup> Thermal properties of their polycondensation products were slightly different to the samples introduced in this work. First, Yao's copolycondensates did not prove double melting response. Second, the

values of  $\chi_c$  were found significantly higher for pure PLA and CA rich samples. Third,  $T_g$  of PLACA samples was lower at higher contents of CA in comparison with Yao's results after recalculation of CA concentrations (Figs. 3 and 5, square symbols). The reason of these variations can be found in the following factors: (a) optical activity of the monomer, LA; (b) slight differences in polycondensation procedure (catalyst, temperature, and pressure); (c) thermal history of the materials. On the other hand, the level of the functionalization [by means of AN (Table I)] was found noticeably higher in our case after recalculation of given parameters within the same units.

Figure 6 shows  $^1\text{H}$  NMR spectra and the ascription of the peaks in the spectra of pure PLA and PLACA polycondensates. On the basis of that, the scheme of the chemical structure of PLACA samples is proposed in Figure 7 together with the structures of monomers. The resonances at 5.16 ppm ( $-\text{CH}$  quartet, b), 1.46 ppm ( $-\text{CH}_3$  doublet, a), 4.2 ppm ( $-\text{CH}$  singlet, hydroxyl end units, c), and at 4.99 ppm ( $-\text{CH}$  singlet, carboxyl end units, d) originate from hydrogen of lactic unit.<sup>29</sup> The resonance of  $\text{CH}_2$  (e) of citric unit of PLACA located in terminal groups appear at 3.0 ppm, but the  $\text{CH}_2$  (f) of citric unit inside the molecular chain of PLACA move to 3.65 ppm. The quartet near 4.05 ppm is contributed by CH (g) of lactic unit connecting with citrate unit. From the  $^1\text{H}$  NMR spectra of PLACA, the mole ratio ( $r$ ) of LA/CA and the number molecular weight of PLACA were calculated according to eqs. (4) and (5), respectively.<sup>21</sup>

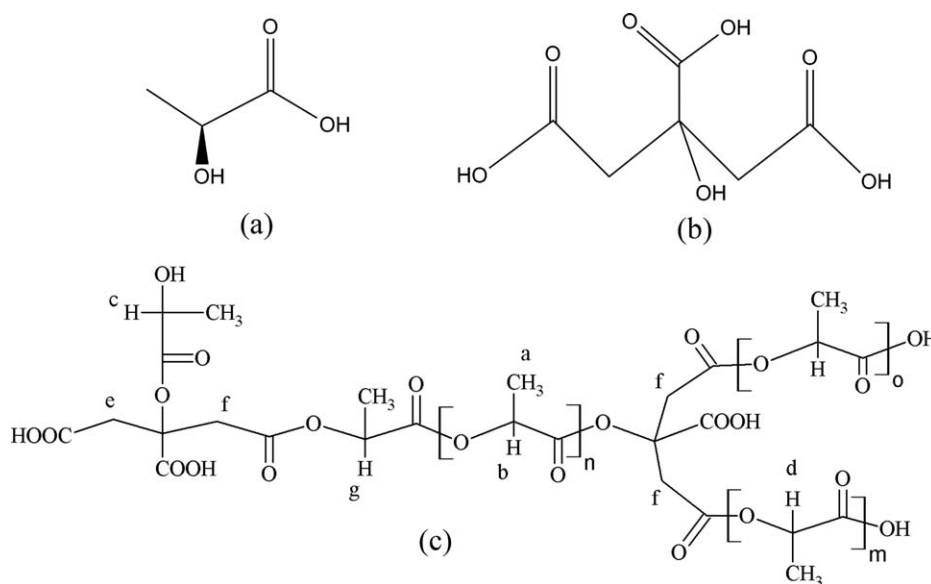


**Figure 7** Schematic structure of (a) LA, (b) CA, and (c) PLACA copolymers.

$$r = \frac{4 \times I_b}{I_f + I_e} \quad (4)$$

$$\overline{M}_n = \frac{I_b}{I_d} \times 72 + \frac{I_b}{I_d} \times \frac{1}{r} \times 158 + 18 \quad (5)$$

where  $I$  represents the integral of the proton signals (peak areas). The calculated results are listed in Table III. The results show that mole ratio of LA/CA ( $r$ ) in PLACA decreases with the increasing concentration of CA in the reaction mixture at the beginning of the polycondensation (see Table IV). From this, it can be concluded that not all CA took part in polycondensation reaction, which was also observed by Yao et al.<sup>21</sup> However, in case of PLACA 1%, the comparison of the  $r$  (Table III) with LA:CA ratio calculated from the known masses of both components introduced into the reactor (LA:CA molar ratio, see Table IV) reveal the significant difference between known LA/CA ratio (211) and  $r$  determined by  $^1\text{H}$  NMR (7690). It could indicate the specific reactions between LA and CA, which occur only at low CA concentrations and do not involve termination of polymer chains mediated by CA units. The value of molecular weight determined by  $^1\text{H}$  NMR (Table III) decreases with increasing content of CA, which is in agreement with the results obtained from GPC anal-

ysis (Table I). Nevertheless, significant discrepancies in the calculated molecular weight values were obtained. The reason can be found in the principles of the  $M_n$  determination and structural features of the polycondensates.

The combination of eqs. (4) and (5) allow the calculation of the molar fraction of the citryl units in 1 mol of PLACA product,  $m_c$  [eq. (6)].<sup>21</sup>

$$m_c = \frac{\overline{M}_n - 18}{158 + 72 r} \quad (6)$$

The values of  $m_c$  increase with the increasing amount of CA in the reaction mixture. On the other hand,  $m_c$  is almost identical for PLACA 5% and PLACA 20% (see Table III). It corresponds to the already proposed limitation of the CA incorporation into the structure of the PLACA polycondensates (inside or at the end of the chains), and it is partially in agreement with AN results presented in Table I.

**TABLE IV**  
Designation of the Samples and Characterization of the Reaction Mixture at the Beginning of the Polycondensation

Sample designation	LA concentration (wt %)	CA concentration (wt/mol %)	LA/CA (molar ratio)
PLA	100	0/0	0
PLACA 1%	99	1/0.47	211
PLACA 3%	97	3/1.43	69
PLACA 5%	95	5/2.41	40
PLACA 7%	93	7/3.41	28
PLACA 10%	90	10/4.95	19
PLACA 15%	85	15/7.64	12
PLACA 20%	80	20/10.49	9

**TABLE III**

Characteristics of PLACA Polycondensates Determined by  $^1\text{H}$  NMR Spectroscopy

Sample designation	$r$	$M_n(\text{kg mol}^{-1})$	$m_c$	$P_{\text{eg}}$
PLA	–	14.4	0	–
PLACA 1%	7690	5.6	0.010	0.80
PLACA 5%	46	0.7	0.197	0.89
PLACA 20%	59	0.8	0.198	0.98



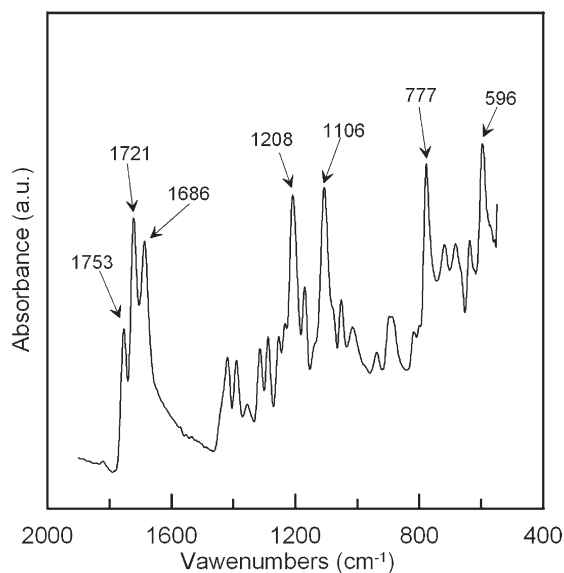


Figure 8 FTIR-ATR spectra of neat CA.

The evidence of CA incorporation inside the PLACA structure could be proved by determination of the percentage of the citryl units,  $P_{eg}$ , located at the end of the chains [eq. (7)].<sup>21</sup>

$$P_{eg} = \frac{2}{3 - \frac{I_f}{I_g}} \times 100 \quad (7)$$

Table III shows the values of  $P_{eg}$ . The results reveal that only 80% of the total present citryl units are located at the ends of the polycondensate's chains. Furthermore,  $P_{eg}$  rises with the increasing CA content in the reaction mixture. It can be considered as an evidence of hypothesis of the CA incorporation inside the structure of the PLACA polycondensates and possible occurrence of the structural inhomogeneities which are connected with that (branching).

The FTIR-ATR spectra of neat CA are shown in Figure 8. CA as tricarboxylic acid has typical absorption peaks positioned at 1753, 1721, and 1686  $\text{cm}^{-1}$  ( $\text{C}=\text{O}$  stretching). It should be mentioned that databases report only two absorption peaks in the region 1800–1650  $\text{cm}^{-1}$ . As can be seen in Figure 7, the intensity of the signal is low, thus the peak at 1753  $\text{cm}^{-1}$  could be considered as random noise signal. Other significant peaks of CA were found at 1208, 1106  $\text{cm}^{-1}$  ( $\text{C}-\text{O}$  stretching) and 777  $\text{cm}^{-1}$  ( $\text{C}-\text{C}$  stretching). Typical FTIR-ATR spectra of the selected samples (PLA, PLACA 1, 5, 10, and 20%) are shown in Figure 9. All spectra prove typical absorptions at 2950  $\text{cm}^{-1}$ , which corresponds to  $\text{C}-\text{H}$  stretching (not presented in Fig. 8). Furthermore, typical PLA absorbance responses were detected at 1748  $\text{cm}^{-1}$  ( $\text{C}=\text{O}$  stretching), 1452  $\text{cm}^{-1}$

( $\text{CH}_3$ - bending), 1381 and 1361  $\text{cm}^{-1}$  ( $\text{C}-\text{H}$  deformations and asymmetric bending), 1267  $\text{cm}^{-1}$  ( $\text{C}-\text{O}$  stretching—typical for PLA prepared by direct polycondensation), 1183, 1128, and 1084  $\text{cm}^{-1}$  ( $\text{C}-\text{O}-\text{C}$  stretching), 1043  $\text{cm}^{-1}$  ( $\text{C}-\text{O}$  bending).<sup>3,8,30</sup> As reported by, e.g., Auras et al., the absorption peaks located at 868 and 753  $\text{cm}^{-1}$  correspond to amorphous and crystalline PLA phase, respectively.<sup>8</sup> The chemical similarities of LA and CA cause difficulties in qualitative analysis of the spectra. The only evidence for a difference can be noticed in the wavenumber region 1700–1600  $\text{cm}^{-1}$  where a slight increase in absorbance can be found. This is evident especially in case of PLACA 20% [Fig. 9(e)]. It could reveal the presence of carboxyl groups (originating from CA) in the structure of the polymer. On the other hand, the evidence of that is expected to be more distinguishable from quantitative analysis of carboxyl group. It was proceeded by comparison of peak areas corresponding to carboxyl groups present in the region 1800–1650  $\text{cm}^{-1}$  ( $A_C$ ), normalized by area of reference peak ( $A_R$ ). The peak at 1452  $\text{cm}^{-1}$  was chosen as internal standard for spectra normalization since it has been reported as suitable for this purpose.<sup>27</sup> The dependence of  $A_C/A_R$  on CA content is shown in Figure 10. It can be noticed that the amount of carboxyl groups grows with increasing concentration of CA in the reaction mixture, which gives evidence for CA units in the polymer structure.

It has been mentioned that FTIR spectra can provide information about the ratio of the crystalline to amorphous phase in the system through observation of the absorption peaks at 868 and 753  $\text{cm}^{-1}$ .<sup>8,10,31</sup> This assumption encouraged us to verify the

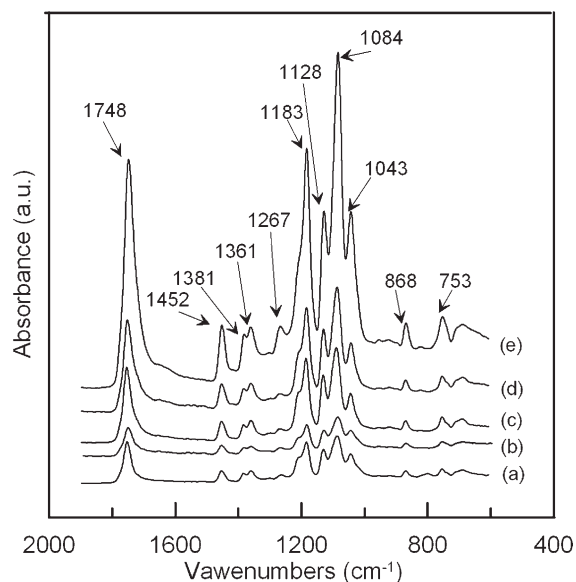
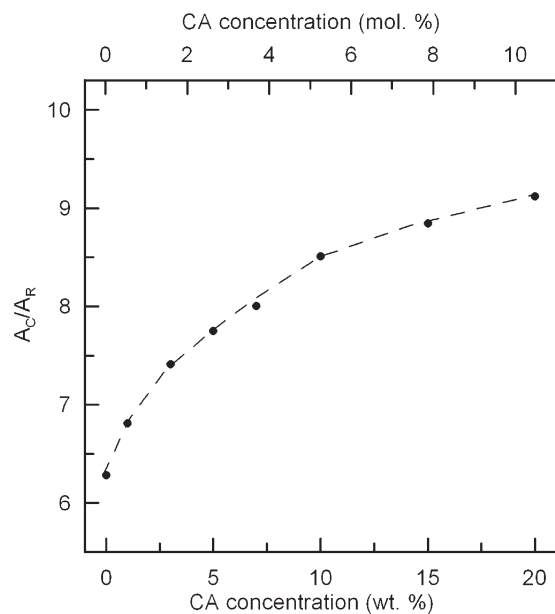
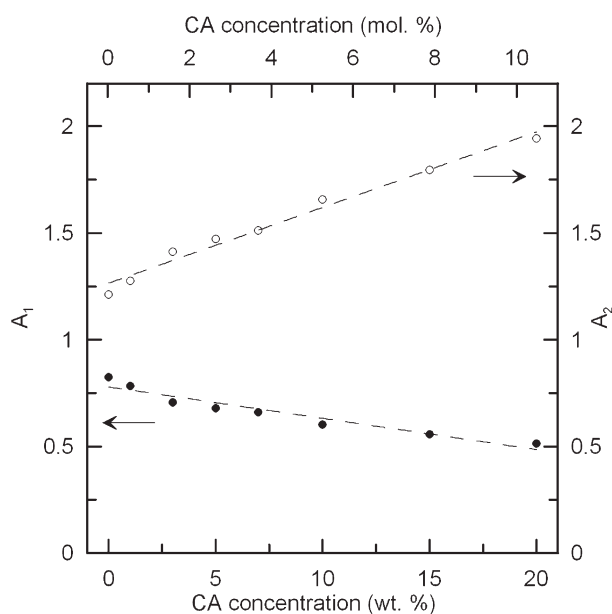


Figure 9 FTIR-ATR spectra of PLA (a), PLACA 1% (b), PLACA 5% (c), PLACA 10% (d), and PLACA 20% (e).



**Figure 10** Correlation of carboxyl groups semiquantitative FTIR determination and concentration of CA in reaction mixture.

authenticity of this theory and compare it with the experimental data obtained from FTIR-ATR and DSC. The normalization of the FTIR-ATR spectra was done in the same way like in case of carboxyl groups analysis; i.e., peak at  $1452\text{ cm}^{-1}$  was considered as the reference.<sup>27</sup> The areas of the discussed peaks  $A_{863}$  and  $A_{753}$  were measured by integration procedure mediated by Omnic Software. The normalized peak areas  $A_1$  ( $A_1 = A_{863}/A_R$ ) and  $A_2$  ( $A_2 = A_{753}/A_R$ ) are depicted against CA concentration in



**Figure 11** Dependence of normalized absorption peak areas on CA concentration ( $A_1 = A_{836}/A_{1452}$  and  $A_2 = A_{753}/A_{1452}$ ).

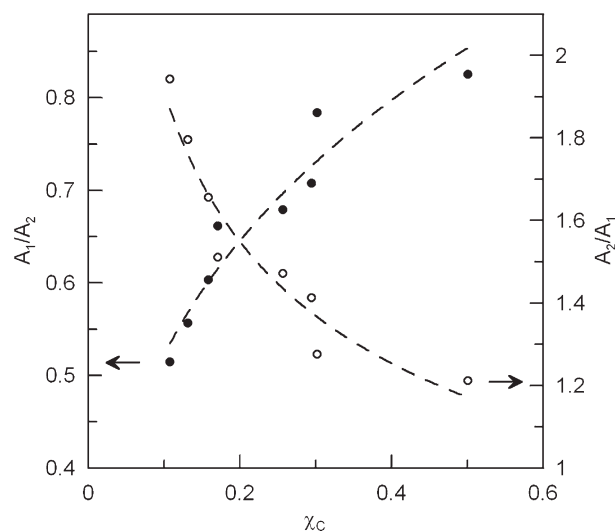


**Figure 12** Correlation between ratios FTIR and DSC results explaining correct assignment of the absorption peaks in PLA-based materials spectra.

Figure 10. The resulting dependences for both  $A_1$  (full symbols) and  $A_2$  (empty symbols) can be fitted by a linear model. The correlation coefficients are 0.96 and 0.99 for  $A_1$  and  $A_2$ , respectively. Figure 11 shows that  $A_1$  decreases with the increasing CA concentration. On the other hand,  $A_2$  proves an opposite trend. These changes are expectable since the peak areas  $A_1$  and  $A_2$  have been reported to express ratio of amorphous ( $A_1$ ) and crystalline ( $A_2$ ) phase of the material and DSC results show significant variation in crystallinity due to the presence of CA in the reaction mixture. However, crystallinity ( $\chi_c$ ) (determined by DSC), which should correspond to  $A_2$ , decreases with the increasing CA concentration. This is evident in Figure 12, where the ratios  $A_1/A_2$  and  $A_2/A_1$  are depicted against  $\chi_c$ . The dependencies were fitted (dashed lines) by a logarithmic model ( $A_1/A_2 = 0.20\ln(\chi_c) + 0.98$ ,  $r = 0.97$ ;  $A_2/A_1 = -0.46\ln(\chi_c) + 0.81$ ,  $r = 0.95$ ). These results indicate the serious discrepancies between previously published data<sup>8</sup> and our results. On the basis of that, it can be concluded that FTIR spectra could be used for PLA crystallinity investigation. However, absorption peak at  $863\text{ cm}^{-1}$  ( $A_1$ ) refers to crystalline and peak at  $753\text{ cm}^{-1}$  ( $A_2$ ) to amorphous phase. Comparison of crystallinity values obtained by FTIR and DSC analysis is shown in Figure 3. Generally, FTIR results provide higher  $\chi_c$  (except for pure PLA) with the significant variance. On the other hand, the trend of  $\chi_c$  reduction corresponds to DSC results.

## CONCLUSIONS

Functionalization of polylactide acid with carboxyl groups, description of the process, finding of limitations, and characterization of the products were

aims of this work. This technique can be used for further preparation of various products with improved bioactive response toward living organisms. This study follows the work, which has been already published by Yao et al.<sup>21</sup> The carboxyl-functionalized copolycondensates LA and CA were prepared by method of direct melt polycondensation.

Generally, the presence of CA in the reaction mixture leads to significant reduction of molecular weight of the polycondensation products. It is believed that CA terminates the growth of the polycondensates chain. We found that the formation of the structures involving citryl units into the polymer chain as well as subsequent branching is possible at low concentrations of CA in the reaction mixtures (up to 1 wt %). The termination processes are predominant at higher CA contents. This effect could be predominant here rather than excess of COOH groups.

The limitations of the CA involving into polycondensation processes have been observed. The AN determinations as well as <sup>1</sup>H NMR spectrometry results show the occurrence of a limit CA concentration (5 wt %). Above this concentration, the functionality degree of the polycondensates is not significantly dependent on CA content. However, the level of functionalization was observed to be noticeably higher in comparison with already published work.<sup>21</sup>

Beside that, the correlation of the data obtained from DSC and FTIR spectroscopy show the possibility of the semiquantitative analysis of the crystalline fraction of the polylactide-based materials.

## References

1. Mehta, R.; Kumar, V.; Bhunia, H.; Upadhyay, S. N. *J Polym Sci.: Polym R* 2005, 45, 325.
2. Ajioka, M.; Suizu, H.; Higuchi, C.; Kashmina, T. *Polym Degrad Stab* 1998, 59, 137.
3. Sedlarik, V.; Saha, N.; Sedlarikova, J.; Saha, P. *Macromol Symp* 2008, 272, 100.
4. Gregorova, A.; Hrabalova, M.; Wimmer, R.; Saake, B.; Altaner, C. *J Appl Polym Sci* 2009, 114, 2616.
5. Jacobsen, S.; Degee, P. H.; Friz, H. G.; Dubouis, P. H.; Jerome, R. *Polym Eng Sci* 1999, 39, 1311.
6. Kricheldorf, H. R. *Chemosphere* 2001, 43, 49.
7. Sedlarik, V.; Kucharczyk, P.; Kasparkova, V.; Drbohlav, J.; Salakova, A.; Saha, P. *J Appl Polym Sci* 2010, 116, 1597.
8. Auras, R.; Harte, B.; Selke, S. *Macromol Biosci* 2004, 4, 835.
9. Duda, A. *Przem Chem* 2003, 82, 905.
10. Garlotta, D. *J Polym Environ* 2001, 9, 63.
11. Sodergard, A.; Stolt, M. *Prog Polym Sci* 2002, 27, 1123.
12. Moon, S. I.; Deguchi, K.; Miyamoto, M.; Kimura, Y. *Polym Int* 2004, 53, 254.
13. Gupta, A. P.; Kumar, V. *Eur Polym Mater* 2007, 43, 4053.
14. Wang, Z. Y.; Zhao, Y. M.; Wang, F. *J Appl Polym Sci* 2006, 102, 577.
15. Popelka, S.; Rypacek, F. *Collect Czech Chem Commun* 2003, 69, 1131.
16. Vesel, A.; Elersic, K.; Junkar, I.; Malic, B. *Mater Technol* 2009, 43, 323.
17. Asadinezhad, A.; Novak, I.; Lehocky, M.; Sedlarik, V.; Vesel, A.; Saha, P.; Chodak, I. *Colloid Surface B* 2010, 77, 246.
18. Asadinezhad, A.; Novak, I.; Lehocky, M.; Bilek, F.; Vesel, A.; Junkar, I.; Saha, P.; Popelka, A. *Molecules* 2010, 15, 2845.
19. Wan, Y.; Tu, C.; Yang, J.; Bei, J.; Wang, S. *Biomaterials* 2006, 27, 2699.
20. Safinia, L.; Datan, N.; Hohse, M.; Mantalaris, A.; Bismarck, A. *Biomaterials* 2005, 26, 7537.
21. Yao, F.; Bai, Y.; Chen, W.; An, X.; Yao, K.; Sun, P.; Lin, H. *Eur Polym Mater* 2004, 40, 1895.
22. Lecorre, P.; Estebe, J. P.; Chevanne, F.; Malledant, F.; Leverage, R. *J Pharm Sci-US* 1995, 84, 75.
23. Norowski, P.A.; Bumgarder, J. D. *J Biomed Mater Res B* 2009, 88B, 530.
24. Vasiliev, A. N.; Gulliver, E. A.; Kninast, J. G.; Riman, R. E. *Surf Coat Technol* 2009, 203, 2841.
25. Cohn, D.; Lando, G. *Biomaterials* 2004, 25, 5875.
26. Yao, F.; Bai, Y.; Zhou, Y.; Liu, C.; Wang, H.; Yao, K. *J Polym Sci: Polym Chem* 2003, 41, 2073.
27. Fischer, E. W.; Sterzel, H. J.; Wegner, G. *Colloid Polym Sci* 1973, 251, 980.
28. Jashimidi, K.; Hyon, S. H.; Ikada, Y. *Polymer* 1998, 29, 2229.
29. Espartero, R. J.; Rashkov, I.; Li, S. M.; Manolova, N.; Vert, M. *Macromolecules* 1986, 29, 3535.
30. Socrates, G. *Infrared Characteristic Group Frequencies*, 2nd ed.; Wiley: Chichester, United Kingdom, 2004, pp 10–17.
31. Kister, G.; Cassanas, G.; Vert, M. *Polymer* 1998, 39, 267.